Journal of Materials Processing Technology 213 (2013) 1900–1907

Contents lists available at ScienceDirect

Journal of Materials Processing Technology

journal homepage: www.elsevier.com/locate/jmatprotec

Friction stir processing of Al/SiC composites fabricated by powder metallurgy

H. Izadi[a,*], A. Nolting[b], C. Munro[b], D.P. Bishop[c], K.P. Plucknett[c], A.P. Gerlich[d]

[a] Department of Chemical and Materials Engineering, University of Alberta, Edmonton, Alberta, Canada T6G 2V4
[b] Defense R&D Canada – Atlantic, Dartmouth, Nova Scotia, Canada B3K 5X5
[c] Department of Process Engineering and Applied Science, Dalhousie University, Halifax, NS, Canada B3J 1Z1
[d] Department of Mechanical and Mechatronics Engineering, University of Waterloo, Waterloo, Ontario, Canada N2L 3G1

ARTICLE INFO

Article history:
Received 20 November 2012
Received in revised form 2 May 2013
Accepted 15 May 2013
Available online 25 May 2013

Keywords:
Metal matrix composite
Powder metallurgy
Friction stir processing

ABSTRACT

Friction stir processing (FSP) was applied to modify the microstructure of sintered Al–SiC composites with particle concentrations ranging from 4 to 16 vol%. Two SiC particle sizes (490N and 800 grades) were examined. Following FSP, the hardness of the 4 and 8 vol% of 490N grade SiC composites increased from 130 HV and 145 HV to 171 HV and 177 HV respectively. The increase was accounted for by the severe deformation occurring during FSP which uniformly distributed the SiC particles. The composites containing 16 vol% SiC could not be fully consolidated using FSP, and contained residual pores and lack of consolidation which originated from the as-received sintered microstructure. The hardness correlated well with the mean inter-particle spacing for the SiC particles in the case of composites containing 4 and 8 vol% SiC.

1. Introduction

Powder metallurgy (PM) is a widely used fabrication method for producing metal matrix composites. This usually involves three major stages: blending of the metal and ceramic powders, pressing or cold compaction, and sintering. These last two steps are often combined during hot pressing. Although PM allows one to produce components with complex geometries in bulk, there are some disadvantages associated with conventional powder metallurgy such as porosity and segregation of the reinforcing particles between the metal matrix particles. This often leads to a degradation of the mechanical properties. These problems become more important when the difference in particle size between the reinforcement and the matrix alloy powders is large or when the volume fraction of the reinforcement is high (Tan and Zhang, 1998).

Rolling, forging or extrusion followed by heat treatment is often applied to eliminate defects such as porosity or particle segregation, and improve the physical and mechanical properties of metal matrix composites produced by powder metallurgy (ASM Metals Handbook, 1992a). For example, the combination of conventional powder metallurgy and extrusion offer several advantages including strengthening due to grain refinement, homogenization of the distribution of the secondary particles, higher productivity, and lower costs (Liu et al., 1994). To this end, Lee et al. have shown that extrusion and forging of a powder metallurgy fabricated Al/SiC composite resulted in an increase from 71 to 430 MPa in tensile strength and an increase from 29 to 103 HV in hardness (Lee et al., 2001), and Smagorinski et al. (1998) have indicated that rolling can completely eliminate pores in PM composites. Liu et al. (2010) have shown that a homogeneous SiC distribution improves yield strength and ultimate tensile strength of Al 2024/SiC composites. The effects of reinforcement particle size and volume fraction on mechanical properties of aluminum matrix composite are also well understood, for example see (Slipenyuk et al., 2006; Uygur, 2004).

Recently friction stir processing (FSP) has been used to post process metal matrix composites produced by different techniques. Morisada et al. (2010) have applied FSP to a thermally sprayed cemented carbide (WC-CrC-Ni) layer in order to eliminate defects and modify the microstructure, resulting in a hardness enhancement of around 1.5 times compared to the as-sprayed composite. Zahmatkesh and Enayati (2010) also showed that the hardness of an Al/Al_2O_3 surface nanocomposite could be increased from 100 to 230 HV due to the enhanced grain refinement of the metal matrix and dispersion of the clusters of nano-sized alumina. An added benefit was also noted, in that bonding of the composite layer to the substrate was improved after FSP. The properties of cast alloys may also be improved by FSP. For example Sun and Apelian (2011) utilized FSP to enhance the microstructure and mechanical properties of an Al–Ta composite. It was noted that after 2 FSP passes the porosity was nearly eliminated and the microstructure was refined with uniformly distributed second phase particles, resulting in higher ductility and strength. In a recent work, Hodder et al. (2013) have used FSP on an Al/Al_2O_3 composite layer produced by cold gas dynamic spraying, in which the alumina particles were

* Corresponding author. Tel.: +17802481997.
E-mail address: hizadi@ualberta.ca (H. Izadi).

0924-0136/$ – see front matter © 2013 H. Izadi. Published by Elsevier B.V. All rights reserved.
http://dx.doi.org/10.1016/j.jmatprotec.2013.05.012

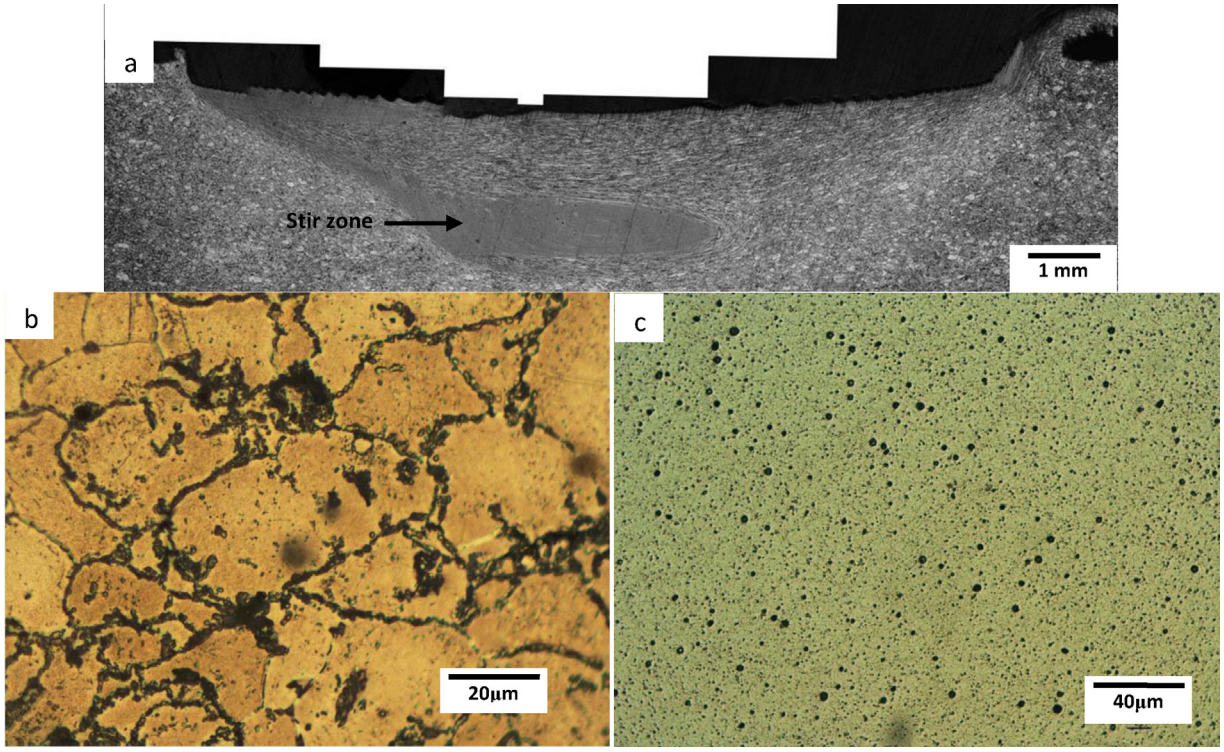

Fig. 1. (a) Microstructure of the sintered and friction stir processed Alumix 431D alloy, with a comparison of (b) the as-sintered and, (c) friction stir processed microstructure.

co-deposited with aluminum powder. It was found that the alumina in the as-sprayed coating became entrapped in between the aluminum particles in the microstructure, but after FSP the alumina was uniformly distributed in the matrix, leading to enhanced hardness. However it remains unclear whether FSP can be effectively used to simultaneously consolidate residual porosity in PM composites materials while also achieving a uniform particle distribution.

Many studies have also examined producing micro and nanoscale composites through FSP directly by processing a groove filled with reinforcing particles (Mishra and Ma, 2005). Although the final properties of the fabricated composites depend on the process parameters (Kurt et al., 2011), but this has been demonstrated as an effective method for distributing various phases in the surface layer of a plate (Kashani-Bozorg and Jazayeri, 2009; Lee et al., 2006; Mahmoud et al., 2008). It has also been demonstrated that metal matrix composites may be joined by friction stir welding (FSW), which is the technology upon which FSP is based (Ceschini et al., 2007; Prado et al., 2003; Wert, 2003). The main feature common to these processes is that the material flow, intermixing, and severe plastic deformation caused by the rotating tool during the FSW/FSP offer a number of benefits when applied to composites. Based on this, the aim of this work is to evaluate effects of FSP on microstructure and mechanical properties of sintered aluminum

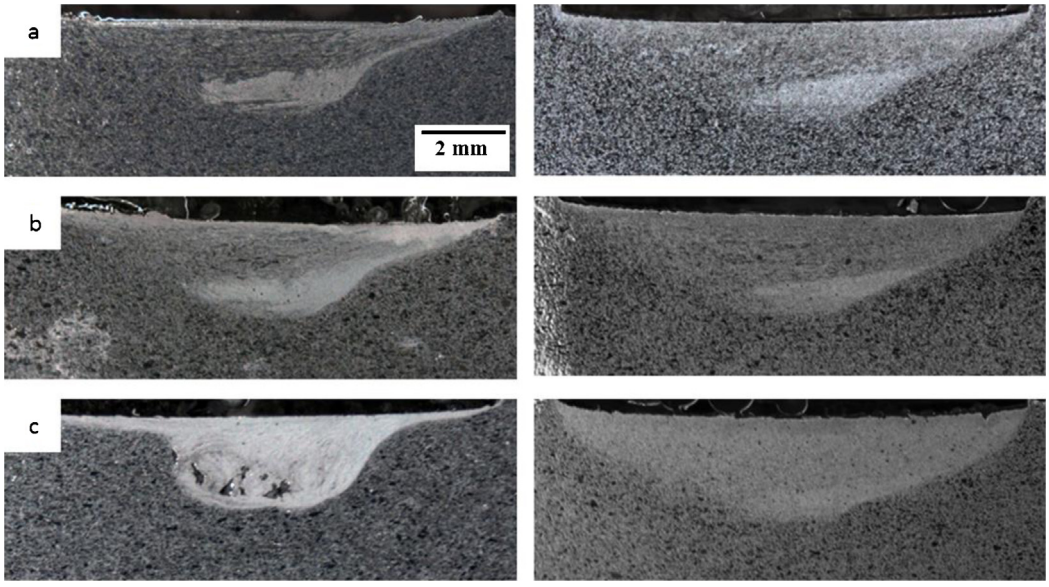

Fig. 2. Macrographs of the FSP samples containing: (a) 4 vol%, (b) 8 vol%, and (c) 16 vol% SiC of 490N grade (left) and 800 grade (right) particle size (same scale for all images).

Table 1
Chemical composition of Alumix 431D.

	Al	Zn	Mg	Cu	Sn	Fe	Mn
Weight%	89.62	5.87	2.52	1.614	0.31	0.06	0.001

metal matrix composites reinforced with different sizes and volume fractions of SiC. The main issues considered are the influence of the particle size and distribution in the processed region.

2. Experimental

The as-received composite samples were produced through powder metallurgy methods by combining Alumix 431D commercial aluminum alloy powder with SiC particles, then de-waxing for 30 min at 400 °C and sintering for 30 min at 605 °C, both in a nitrogen environment. Table 1 shows the composition of Alumix 431D, which is intended to be a heat treatable powder metallurgy alloy with similar chemistry and hardness to Al 7075. Two grades of SiC particles were used which had average particle sizes (d_{50} values representing the 50th percentile in size distribution) of 0.61 μm and 6.25 μm, and these will be referred to as 490N and 800 grade, respectively. The two grades of SiC were added to the aluminum powder at 4, 8 and 16 volume percentages. Friction stir processing was performed on each sample with a tool having a tapered and threaded pin (with an M4 profile, or 0.7 mm pitch) which was 4 mm at the end, and 5.1 mm at the base, with three flats separated by 120°, as shown in a previous work (Gerlich et al., 2009). The shoulder had a 12 mm diameter, and processing was conducted with a tool rotation speed of 454 rpm and travel speed of 88 mm/min. To minimize tool wear the tool was coated with a multilayered structure of alternating layers of vapour deposited TiN/ZrN. The microstructure of all samples before and after FSP was studied using optical microscopy and scanning electron microscopy (SEM). To do this, samples were prepared using conventional metallographic

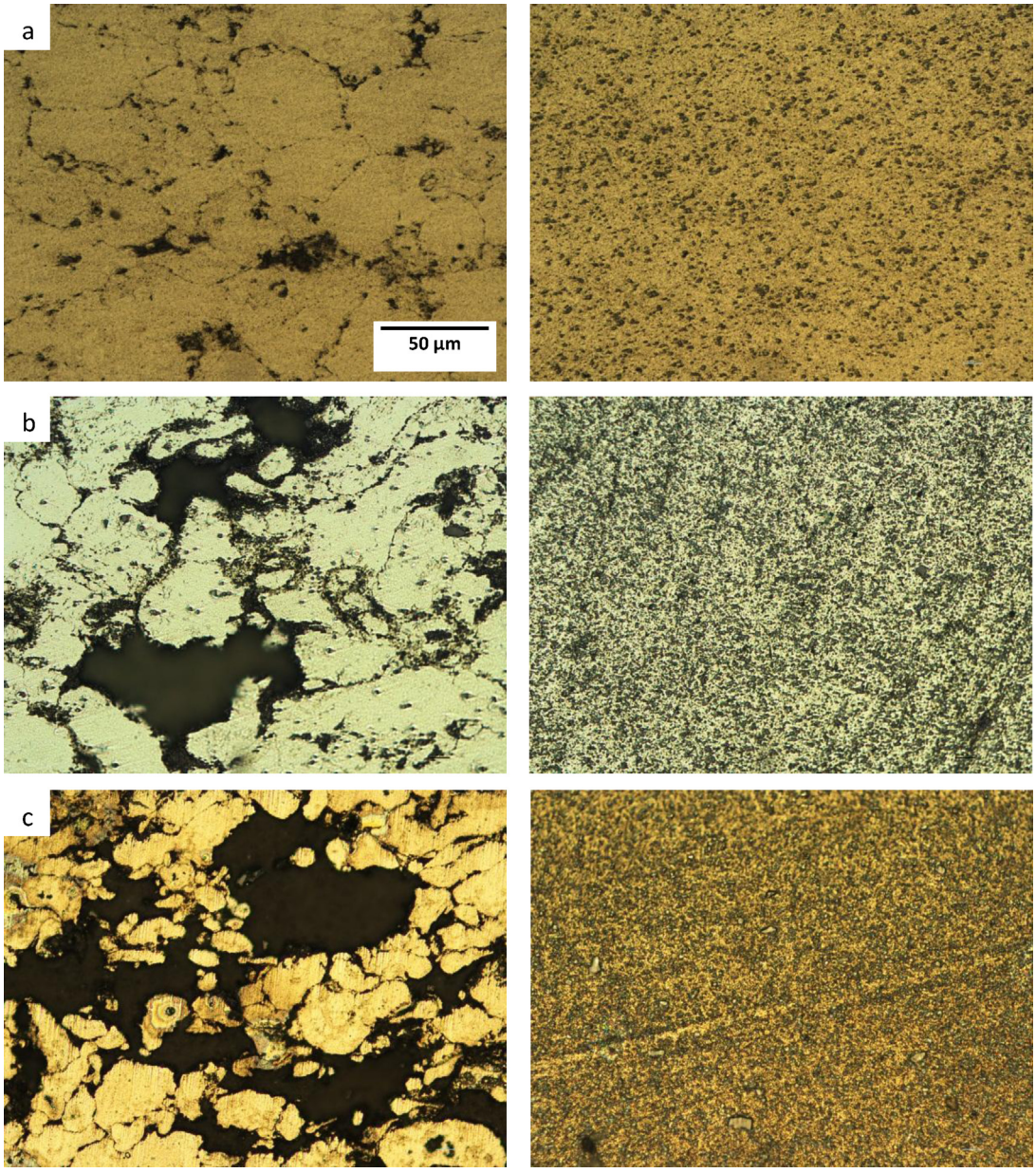

Fig. 3. Grade 490N samples containing: (a) 4 vol%, (b) 8 vol%, and (c) 16 vol% SiC in as-sintered (left) and friction stir processed (right) conditions (same scale for all images).

Table 2
Theoretical and measured density of the samples after compaction and before sintering.

SiC particle grade	Vol% SiC	Theor. density (g/cm^3)	Measured density (g/cm^3)	Relative density (%)	Std. dev. (%)
800	4	2.826	2.473	87.5	0.02
800	8	2.842	2.453	86.3	0.04
800	16	2.874	2.409	83.8	0.11
490N	4	2.826	2.444	86.5	0.03
490N	8	2.842	2.416	85.0	0.29
490N	16	2.874	2.343	81.5	0.05

sample preparation procedures, followed by electrolytic polishing for 75 s in 3% HBF_4. Microstructure of all samples was examined in the as-polished (not etched) condition. SEM was conducted using either a Zeiss EVO MA 15 or a Vega-3 Tescan machine. To measure the inter-particle spacing five pictures of each sample were selected before and after FSP, and the reported measurements are the averages of several calculations on each picture. A Mitutoyo MVK – H1 hardness tester set at 500 g was used to determine the Vickers microhardness of the sample across the stir zone region.

3. Results and discussion

In the case of sintered powder composites, it is well known that some porosity is always present, and this usually increases with the addition of secondary hard particles. The microstructure of the sintered Alumix 431D alloy (without SiC) is shown in Fig. 1, before and after FSP. The refinement of the stir zone microstructure after friction stir processing is evident in comparing Fig. 1b and c, and it can also be noted that the inter-particle porosity is absent after FSP.

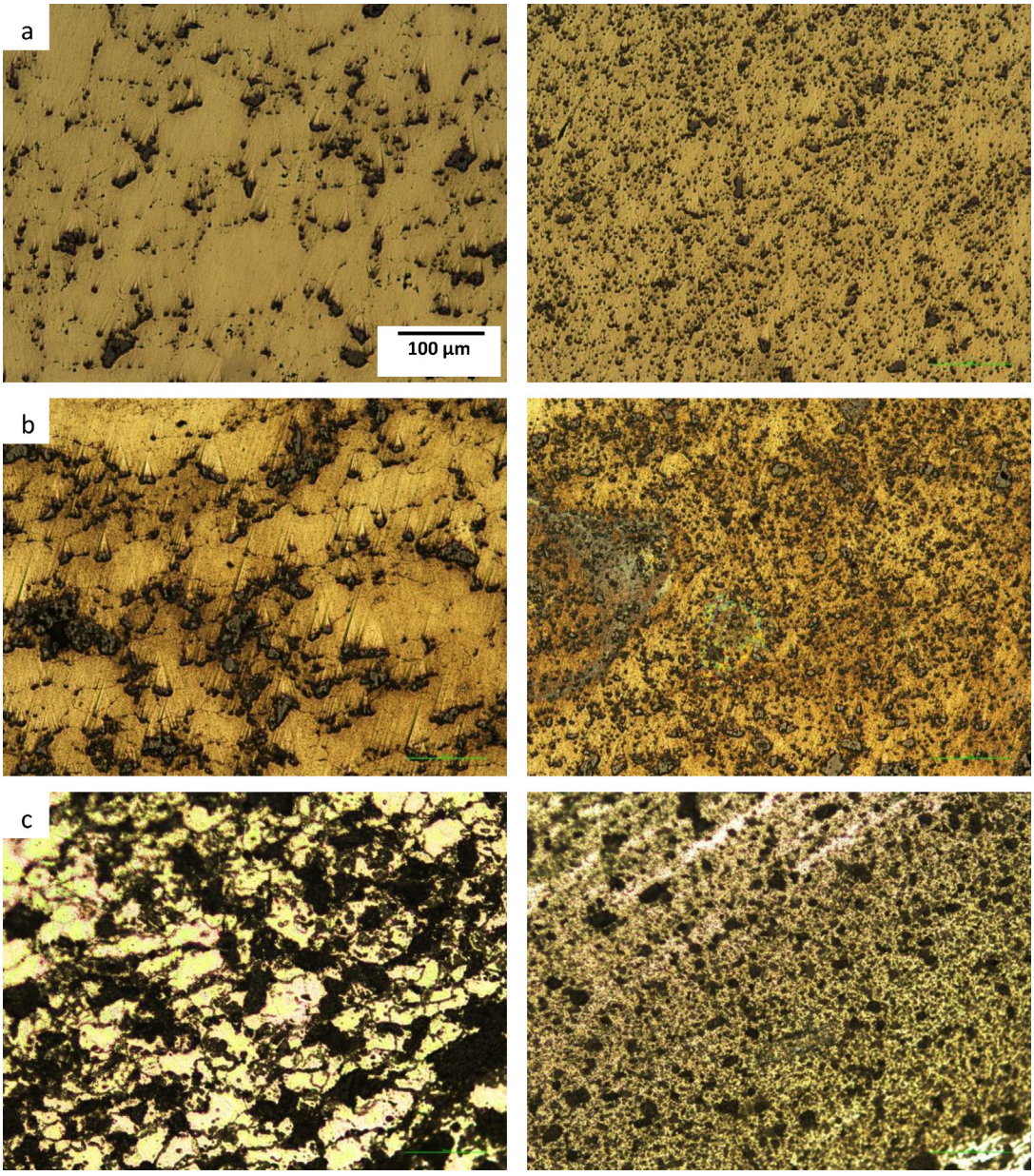

Fig. 4. Grade 800 samples containing: (a) 4 vol%, (b) 8 vol%, and (c) 16 vol% SiC in as-sintered (left) and friction stir processed (right) conditions (same scale for all images).

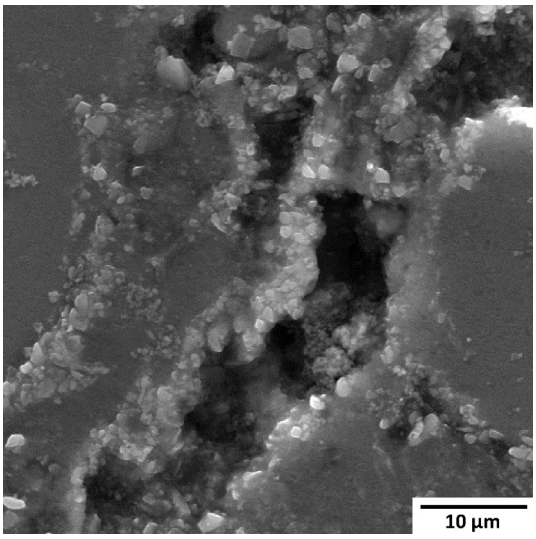

Fig. 5. SEM micrograph of porosity and SiC clusters at the aluminum alloy-particle interface in the Al-8 vol% SiC (grade 490N) composite.

The typical porosity occurring in the as-sintered condition is often the result of poor powder mixing (Liu et al., 1994) or insufficient compaction and sintering conditions (Huei-Long et al., 1992).

Cross-sections of the samples modified by FSP with different volume fractions and particle sizes of SiC are shown in Fig. 2. Some indications of the material flow caused by FSP can also be observed in Fig. 2 and will be discussed later. There are also indications that the refined structure dominated more of the lower stir zone region, and the asymmetry between the advancing and retreating side remains.

Figs. 3 and 4 show microstructures of the as-sintered and friction stir processed samples containing 4, 8, and 16 vol% 490N and 800 grade SiC particles, respectively. Micrographs of processed samples were obtained from the center of the stir zone, as indicated in Fig. 1a for the sintered Alumix 431D. Comparing the as-sintered microstructure of samples reveals that segregation of SiC particles, as well as the volume fraction and size of pores, increases with increasing fractions of SiC. The higher fraction of reinforcing particles causes clustering of SiC which leads to difficulty in compaction and sintering, resulting in a higher fraction of porosity. In such cases pores are mostly located in SiC clusters, as illustrated by SEM microscopy in Fig. 5. In this regard Slipenyuk et al. have defined a critical content for SiC in powder metallurgy Al–SiC composites based on the properties of the matrix and reinforcement powders. They have suggested that increasing the volume fraction of SiC above a critical value of 7.6 vol% will cause an increase in volume fraction of pores and heterogeneity. However, it should be noted that this exact value is dependent on the size and shape of the particles used (Slipenyuk et al., 2006).

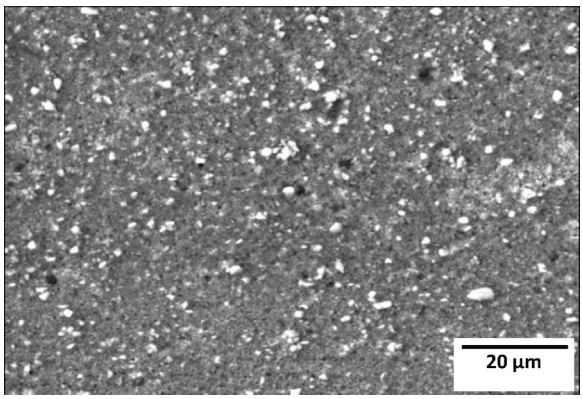

Fig. 7. SEM micrograph of stir zone region in friction stir processed Al-8 vol% SiC (grade 490N) composite.

The SiC particle size also affects the amount and size of pores remaining after sintering. Smaller particles have higher specific surface area which leads to an increase in the amount of porosity during compaction and sintering. In addition higher specific surface area leads to higher inter-particle friction, resulting in poor particle distribution (Rahimian et al., 2010; Razavi-Tousi et al., 2011; Slipenyuk et al., 2006). This may account for why the composite sintered using 16 vol% 490N grade SiC powder could not be fully consolidated, in which case the stir zone contained cracks and voids, as shown in Fig. 6. On the other hand, it can be seen in Fig. 2 that for the sample with 16 vol% 800 grade SiC powder the consolidation problem is less pronounced since larger particles are used. Therefore it is suggested that the small size and high volume fraction of SiC particles led to the high initial porosity in the as-sintered material, which could not be consolidated using the FSP processing parameters applied. The influence of secondary particles size and volume fraction on amount of porosity after compaction and before sintering is shown in Table 2, where the theoretical density values are based on the density for the aluminum alloy reported by LaDelpha et al. (2009). As discussed above it can be seen that the relative density decreases with increasing volume fractions of particles, and slightly decreases with SiC particle size as well. It is also clear from Fig. 4 that the average size of the grade 800 SiC particles was significantly refined during FSP, and this is consistent with prior studies (Cavaliere, 2005; Mahmoud et al., 2008).

Fig. 7 shows the microstructure of the stir zone region in friction stir processed Al-8 vol% SiC (grade 490N) composite. It is clear that the distribution of the SiC particles is uniform after one FSP pass. Another aspect to consider is the refinement of the SiC particles which occurs during FSP. This has been observed during friction stir welding/processing of different composites (Bozkurt

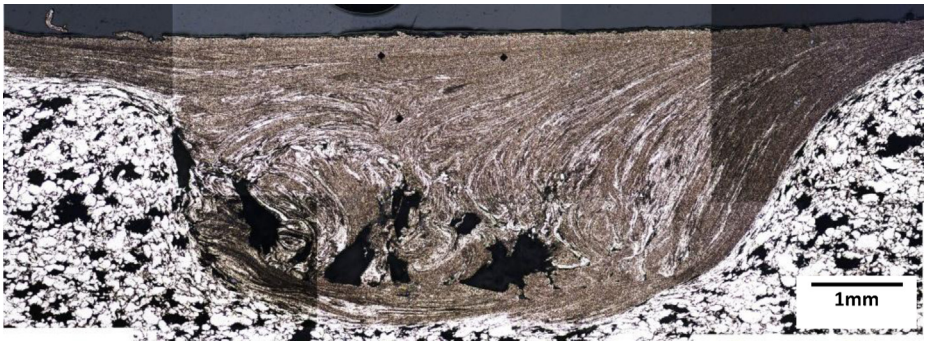

Fig. 6. Microstructure of sample containing 16 vol% of 490N grade SiC particles; large pores are visible in the stir zone.

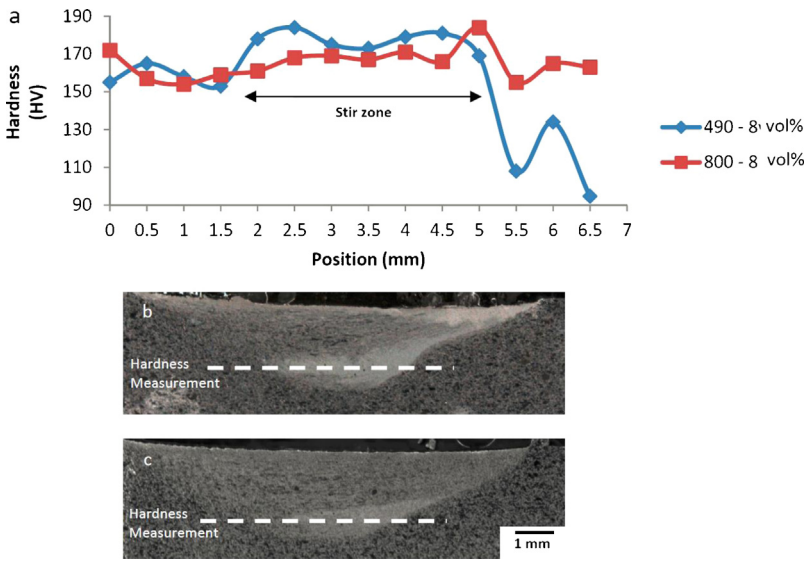

Fig. 8. (a) Microhardness distribution across stir zone, for friction stir processed Al/8 vol% SiC using (b) 490N and (c) 800 grade SiC powders.

et al., 2011; Mahmoud et al., 2009; Su et al., 2006). Jun et al. (2008) have reported that the size of alumina particles from a range of 10–50 μm is ultimately refined to a range of 1–5 μm following FSP of Al 1100/Al_2O_3 composites, and indicated that particle fragmentation increases by increasing rotation speed or decreasing travel speed. Some refinement of the SiC particles can similarly be expected due to the shearing forces and attrition imposed within the stir zone region during FSP, and this will lead to a reduction in the average inter-particle spacing.

The microhardness distribution across the stir zone region is indicated in Fig. 8 for the processed samples containing 8 vol% SiC, using both the 490N and 800 grades. The transfer of material by the tool toward the advancing side (right side in the micrograph) is clearly observed, and the lower portion of the stir zone (appearing light) contains the most uniformly distributed SiC particles, as also shown in Fig. 2. This may be explained by the material flows that are imposed during friction stir welding (Gerlich et al., 2008; Su et al., 2007), which promote redistribution due to the recirculation of material caused by the presence of tool threads. The hardness distribution was quite uniform across the stir zone region, which had homogeneous distribution of the SiC particles as shown in Fig. 8. The hardness of the fine grained material in the middle of the stir zone (from positions 2 to 5 mm in Fig. 8a) was an average of 177 ± 4.7 HV in the sample containing 490N grade SiC, compared to 169.5 ± 6.6 HV for the sample produced using the coarser 800 grade particles. A great deal of scatter in the hardness measurements is observed in the base material due to the presence of residual porosity.

The average hardness increased significantly in the stir zone compared to the as-sintered composites, as shown in Fig. 9. It should be noted that the as-sintered material contained significant porosity, and an attempt was made to avoid pores, consequently the macro-scale hardness could potentially be lower than these measured results. However, the Alumix 431D alloy had a hardness of 139 ± 4.7 HV in the as-sintered condition, and 155 ± 1.3 HV after FSP. In the case of the material containing 16 vol% SiC, the rate of porosity in the as-received samples introduced difficulty in

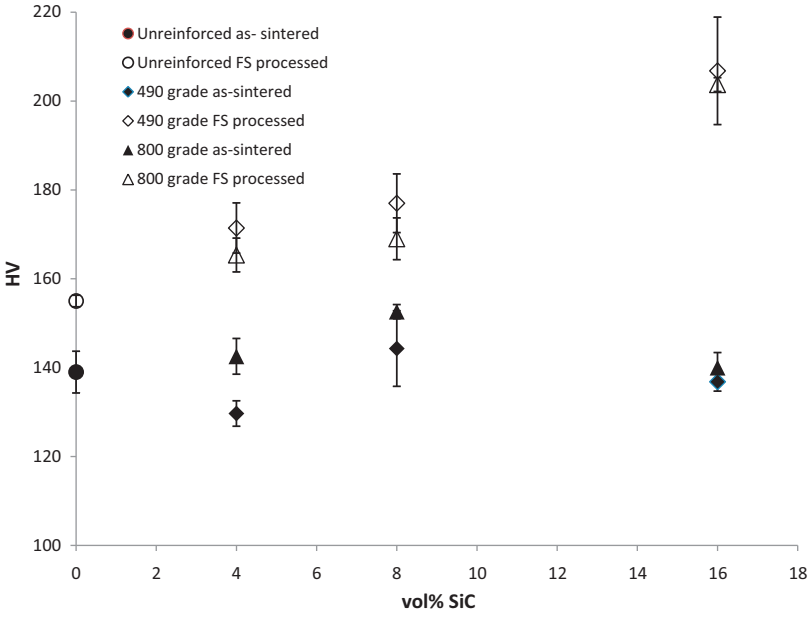

Fig. 9. Microhardness values of the sintered Al–SiC composites modified by FSP.

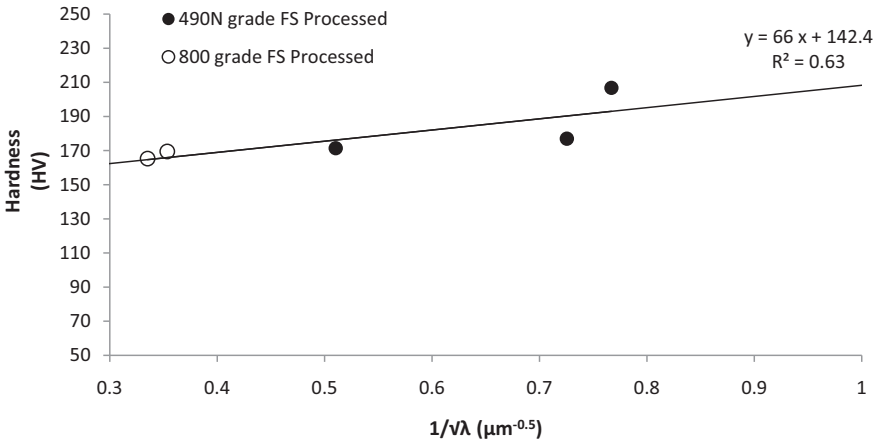

Fig. 10. Variation of hardness with inter-particle spacing for the friction stir processed composite samples.

obtaining clear Vickers hardness measurements due to the indentation marks being obscured or landing on pores. The reported values are the average of hardness values obtained from indentations on pore-free regions; therefore they are higher than the actual hardness of the as-sintered sample which contains a considerable amount of porosity. The finer particle size in the samples made using 490N grade SiC did not appear to provide a significant difference in hardness in the composite after FSP, since the difference in particle sizes was reduced by the significant refinement of the 800 grade particles. This suggests that differences observed between the as-sintered composites for the two grades of SiC likely stem from both the particle size difference, and variation in residual porosity of the samples.

The homogenous SiC particle redistribution obtained as a result of stirring and mixing caused by the tool during FSP has been previously reported during composite fabrication via FSP (Mahmoud et al., 2008). This improvement of secondary particle dispersion can be quantified and related to mechanical properties by the concept of inter-particle spacing, λ, which is the distance between adjacent particles calculated using the following formula:

$$\lambda = \frac{1 - V_p}{N_L} \quad (1)$$

where V_p is the volume fraction of particles and N_L is the number of particle intercepts per unit length of test line. As discussed above, for as-sintered samples the majority of particles were agglomerated in the boundary regions between the original aluminum particles, and samples contained a large fraction of porosity. Consequently, it is not meaningful to compare the inter-particle spacing values for the as-sintered samples, but only for the samples subjected to FSP where the porosity was eliminated and a uniform particle distribution was achieved. This approach has been previously used by Hodder et al. (2013) when examining Al/Al_2O_3 composites fabricated using a combination of cold spraying and FSP. In Fig. 10 the inter-particle spacing value, λ, is plotted against the hardness values for the FSP composites made using different volume fractions of SiC. In the case of the samples made using 16 vol% of 800 grade SiC the amount of porosity was very high (as shown in Fig. 4), making it impossible to recognize the particles and compare the inter-particle spacing.

As the inter-particle spacing decreases with increasing particle volume fraction, the hardness also increases. This enhancement is attributed to the elevated degree of particle–matrix interaction during hardness testing (see Fig. 10). Such a relation has been previously reported between yield strength and $1/\sqrt{\lambda}$ of different metal matrix composites (Gustafson et al., 1997; Lee et al., 1998). On the other hand, Kouzeli and Mortensen (2002) have shown that the matrix yield strength is proportional to $1/\lambda$, and also noted that when B_4C is compared to Al_2O_3 as a reinforcing particle in pure aluminum a higher degree of strengthening is observed in the slope of the strength versus $1/\lambda$ curve. The enhanced strengthening was explained as a consequence of the greater mismatch between the coefficients of thermal contraction, which produces a greater number of geometrically necessary dislocations on cooling from high temperature sintering when B_4C is used.

When a similar analysis is applied here the slope of the curve in Fig. 9 also indicates the effectiveness of the SiC particles in hardening the matrix. The slope of 66 shown in Fig. 10 is lower than that observed in prior work examining pure Al reinforced with Al_2O_3, where the slope relating hardness and $1/\sqrt{\lambda}$ was 100.9 (Hodder et al.). This result was interesting, considering that the mismatch between the coefficients of thermal contraction in aluminum alloys is far greater for SiC than Al_2O_3 (ASM Metals Handbook, 1992b). This may be explained by the fact that when different matrix alloys are compared, the contribution of work hardening in the Alumix 431D alloy (which contains significant alloying additions and undergoes precipitation strengthening (LaDelpha et al., 2009)) might not be as significant as in the case of pure aluminum based metal matrix composites studied in prior works (Hodder et al., 2013; Kouzeli and Mortensen, 2002). In addition, it should also be noted that the peak temperature during FSP is below the melting point of the alloy, and hence the effect of thermal stresses during contraction following processing may be suppressed compared to other composite fabrication techniques. However, it should be considered that the Alumix 431D-SiC composite achieved a much higher overall hardness (160–205 HV depending on the SiC content) compared to the Al–Al_2O_3 or Al–B_4C composites, even though the concentration of reinforcing particles was lower. It is therefore likely that the matrix alloy contributes to the hardness as well due to solution strengthening and possible precipitation at room temperature following FSP. Compared to the as-sintered composites the hardness values following FSP increased with SiC fraction, since the distribution of the reinforcement was much more uniform, particle agglomerations were dispersed, and porosity decreased. It should also be considered that other mechanisms such as grain refinement of the metal matrix during FSP may also contribute to the enhanced hardness values measured in the stir zones.

4. Conclusions

The use of FSP has been shown to improve the microhardness of Al–SiC composites produced by traditional powder metallurgy and sintering methods. The material flow in the stir zone during FSP was successful in uniformly distributing the SiC particles.

However, when samples with 16 vol% SiC were processed there were residual pores and lack of consolidation. This was likely due to the initial low density (81.5–83.8% of theoretical) in the compacted materials, which could be attributed to the larger surface area of the fine particles used. An increase in hardness of all samples was observed after friction stir processing which was attributed to the improvement in particle distribution and elimination of porosity. Some refinement of the initial SiC particles appeared to occur and it was shown that the influence of reducing the initial SiC particle size on hardness values of the friction stir processed samples was negligible. The increase in hardness with SiC concentration in the friction stir processed samples appeared to be related to the mean inter-particle spacing. In this regard, a possible quantitative linear correlation has been proposed.

Acknowledgments

This project was financially supported by Natural Sciences and Engineering Research Council of Canada (NSERC) and Defense R&D Canada. The authors acknowledge Joyce Lam for assistance with sample preparation.

References

ASM Metals Handbook, 1992a. Volume 2: Properties and Selection: Nonferrous Alloys and Special-Purpose Materials. ASM International.

ASM Metals Handbook, 1992b. Volume 7: Powder Metals Technologies and Applications. ASM International.

Bozkurt, Y., Uzun, H., Salman, S., 2011. Microstructure and mechanical properties of friction stir welded particulate reinforced AA2124/SiC/25p-T4 composite. Journal of Composite Materials 45, 2237–2245.

Cavaliere, P., 2005. Mechanical properties of friction stir processed 2618/Al_2O_3/20p metal matrix composite. Composites Part A: Applied Science and Manufacturing 36, 1657–1665.

Ceschini, L., Casagrande, A., Minak, G., Morri, A., Tarterini, F., 2007. Microstructural and mechanical characterization of friction stir welded joints of an A6061/20%vol Al_2O_3p composite. Composites Part A: Applied Science and Manufacturing 38, 1200–1210.

Gerlich, A., Su, P., Yamamoto, M., North, T.H., 2008. Material flow and intermixing during dissimilar friction stir welding. Science and Technology of Welding and Joining 13, 254–264.

Gerlich, A., Yamamoto, M., Shibayanagi, T., North, T.H., 2009. Selection of welding parameter during friction stir spot welding. SAE International Journal of Materials and Manufacturing 1, 1–8.

Gustafson, T.W., Panda, P.C., Song, G., Raj, R., 1997. Influence of microstructural scale on plastic flow behavior of metal matrix composites. Acta Materialia 45, 1633–1643.

Hodder, K.J., Izadi, H., McDonald, A.G., Gerlich, A.P., 2013. Fabrication of aluminum–alumina metal matrix composites via cold gas dynamic spraying at low pressure followed by friction stir processing. Materials Science and Engineering: A 556, 114–121.

Huei-Long, L., Wun-Hwa, L., Sammy Lap-Ip, C., 1992. Abrasive wear of powder metallurgy Al alloy 6061-SiC particle composites. Wear 159, 223–231.

Jun, Q., Zhili, F., Hanbing, X., Frederick, D.A., Jolly, B.C., David, S.A., 2008. Producing a Composite Surface Using Friction Stir Processing, Seattle, WA., pp. 33–36.

Kashani-Bozorg, S.F., Jazayeri, K., 2009. Formation of Al/B_4C Surface Nano-Composite Layers on 7075 Al Alloy Employing Friction Stir Processing, Selangor., pp. 715–719.

Kouzeli, M., Mortensen, A., 2002. Size dependent strengthening in particle reinforced aluminium. Acta Materialia 50, 39–51.

Kurt, A., Uygur, I., Cete, E., 2011. Surface modification of aluminium by friction stir processing. Journal of Materials Processing Technology 211, 313–317.

LaDelpha, A.D.P., Neubing, H., Bishop, D.P., 2009. Metallurgical assessment of an emerging Al-Zn-Mg-Cu P/M alloy. Materials Science and Engineering A 520, 105–113.

Lee, C.J., Huang, J.C., Hsieh, P.J., 2006. Mg based nano-composites fabricated by friction stir processing. Scripta Materialia 54, 1415–1420.

Lee, H.S., Yeo, J.S., Hong, S.H., Yoon, D.J., Na, K.H., 2001. The fabrication process and mechanical properties of SiCp/Al-Si metal matrix composites for automobile air-conditioner compressor pistons. Journal of Materials Processing Technology 113, 202–208.

Lee, J., Kim, N.J., Jung, J.Y., Lee, E.S., Ahn, S., 1998. The influence of reinforced particle fracture on strengthening of spray formed Cu-TiB 2 composite. Scripta Materialia 39, 1063–1069.

Liu, Y.B., Lim, S.C., Lu, L., Lai, M.O., 1994. Recent development in the fabrication of metal matrix-particulate composites using powder metallurgy techniques. Journal of Materials Science 29, 1999–2007.

Liu, Z.Y., Wang, Q.Z., Xiao, B.L., Ma, Z.Y., Liu, Y., 2010. Experimental and modeling investigation on SiCp distribution in powder metallurgy processed SiCp/2024 Al composites. Materials Science and Engineering: A 527, 5582–5591.

Mahmoud, E.R.I., Ikeuchi, K., Takahashi, M., 2008. Fabrication of SiC particle reinforced composite on aluminium surface by friction stir processing. Science and Technology of Welding and Joining 13, 607–618.

Mahmoud, E.R.I., Takahashi, M., Shibayanagi, T., Ikeuchi, K., 2009. Effect of friction stir processing tool probe on fabrication of SiC particle reinforced composite on aluminium surface. Science and Technology of Welding and Joining 14, 413–425.

Mishra, R.S., Ma, Z.Y., 2005. Friction stir welding and processing. Materials Science and Engineering R: Reports, 50.

Morisada, Y., Fujii, H., Mizuno, T., Abe, G., Nagaoka, T., Fukusumi, M., 2010. Modification of thermally sprayed cemented carbide layer by friction stir processing. Surface and Coatings Technology 204, 2459–2464.

Prado, R.A., Murr, L.E., Soto, K.F., McClure, J.C., 2003. Self-optimization in tool wear for friction-stir welding of Al 6061+20% Al_2O_3 MMC. Materials Science and Engineering A 349, 156–165.

Rahimian, M., Parvin, N., Ehsani, N., 2010. Investigation of particle size and amount of alumina on microstructure and mechanical properties of Al matrix composite made by powder metallurgy. Materials Science and Engineering A 527, 1031–1038.

Razavi-Tousi, S.S., Yazdani-Rad, R., Manafi, S.A., 2011. Effect of volume fraction and particle size of alumina reinforcement on compaction and densification behavior of Al-Al_2O_3 nanocomposites. Materials Science and Engineering A 528, 1105–1110.

Slipenyuk, A., Kuprin, V., Milman, Y., Goncharuk, V., Eckert, J., 2006. Properties of P/M processed particle reinforced metal matrix composites specified by reinforcement concentration and matrix-to-reinforcement particle size ratio. Acta Materialia 54, 157–166.

Smagorinski, M.E., Tsantrizos, P.G., Grenier, S., Cavasin, A., Brzezinski, T., Kim, G., 1998. The properties and microstructure of Al-based composites reinforced with ceramic particles. Materials Science and Engineering A 244, 86–90.

Su, P., Gerlich, A., North, T.H., Bendzsak, G.J., 2006. Material flow during friction stir spot welding. Science and Technology of Welding and Joining 11, 61–71.

Su, P., Gerlich, A.P., North, T.H., Bendzsak, G.J., 2007. Intermixing in dissimilar friction stir spot welds. Metallurgical and Materials Transactions A 38 A, 584–595.

Sun, N., Apelian, D., 2011. Friction stir processing of aluminum cast alloys for high performance applications. JOM 63, 44–50.

Tan, M.J., Zhang, X., 1998. Powder metal matrix composites: Selection and processing. Materials Science and Engineering A 244, 80–85.

Uygur, I., 2004. Tensile behavior of powder metallurgy processed Al-Cu-Mg-Mn/SiCp composites. Iranian Journal of Science and Technology, Transaction B: Engineering 28, 239–248.

Wert, J.A., 2003. Microstructures of friction stir weld joints between an aluminium-base metal matrix composite and a monolithic aluminium alloy. Scripta Materialia 49, 607–612.

Zahmatkesh, B., Enayati, M.H., 2010. A novel approach for development of surface nanocomposite by friction stir processing. Materials Science and Engineering A 527, 6734–6740.